Pergamon

PII: S0038-092X(96)00006-0

Solar Energy Vol. 56, No. 6, pp. 513–520, 1996

0038-092X/96 \$15.00+0.00

NUMERICAL SIMULATION OF CURRENT–VOLTAGE CHARACTERISTICS OF PHOTOVOLTAIC SYSTEMS WITH SHADED SOLAR CELLS

VOLKER QUASCHNING† and ROLF HANITSCH†
Electrical Machines Institute, Berlin University of Technology, Secretariat EM 4, Einsteinufer 11, D-10587 Berlin, Germany

(Communicated by JOACHIM LUTHER)

Abstract—In photovoltaics the actual curve of the current–voltage characteristic of a solar generator is often needed, for example if the maximum power point is to be determined. It is convenient to use a model for the description of the relationship between current and voltage, which is able to describe the solar cell in the generation region as well as the breakdowns at positive and negative voltages. As the mathematical expression cannot be given in an explicit form, a set of suitable numerical algorithms to compute the currents for a given voltage and vice versa is given. For more complex solar generators, it can neither be assumed that the solar cells have identical electrical characteristics, nor that they are evenly illuminated. A general model for the description of solar generators is proposed that gives all voltages and currents as well as the voltage and current at the outputs of the solar generator itself. This new model is also implemented in a numerical algorithm. The characteristics of partially shaded solar generators were calculated and discussed using the proposed models. Copyright © 1996 Elsevier Science Ltd.

1. INTRODUCTION

For the description of the electrical behavior of a solar cell the two diodes model is commonly used, see e.g. Overstraeten (1986).

For cells that are driven in the negative voltage range another model is necessary, which describes the breakdown region at high negative voltages. Negative voltages for solar cells can occur at non-uniform illuminated photovoltaic generators, especially during partial shading of the generator. One model was described by Rauschenbach (1980). A more precise model, based on the one diode model, was given by Bishop (1988). This model can be adapted to the two diodes model and offers optimal conditions for the description of the solar cell characteristics.

Several simulation programs for photovoltaic generators were developed during the last two decades. Due to the development of more powerful computers, they became more complex and more efficient. These programs, however, still offer limited possibilities to simulate the electrical behavior of photovoltaic generators under mismatched conditions or partial shading. For this purpose, a more general electrical model which allows simulations at all conditions has been developed. Numerical methods, such as described by Press *et al.* (1992) are used to obtain a solution for this model.

†ISES member.

2. SOLAR CELL MODEL

The two diodes model is widely used for an equivalent circuit. Shaded cells of a solar module or a solar generator can be driven into the negative voltage region. If there are no bypass diodes for cell protection, a diode breakdown may happen during high negative voltages. This breakdown is not taken into account in the two diodes model. Therefore another model is described in this paper.

This model includes an extension term, which describes the diode breakdown at high negative voltages. The equivalent of this model is given in Fig. 1.

Kirchhoff's first law yields the following relationship between cell current and cell voltage:

$$\begin{aligned}0 &= f(V,I)\\ &= I_{\mathrm{Ph}} - I_{\mathrm{S1}}\left(\exp\left(\frac{V+IR_{\mathrm{S}}}{m_1 V_{\mathrm{T}}}\right)-1\right)\\ &\quad - I_{\mathrm{S2}}\left(\exp\left(\frac{V+IR_{\mathrm{S}}}{m_2 V_{\mathrm{T}}}\right)-1\right) - \frac{V+IR_{\mathrm{S}}}{R_{\mathrm{P}}}\\ &\quad - I - \underbrace{a(V+IR_{\mathrm{S}})\left(1-\frac{V+IR_{\mathrm{S}}}{V_{\mathrm{Br}}}\right)^{-n}}_{\text{Extension term for the negative diode breakdown}} \qquad (1)\end{aligned}$$

This equation differs from the usual two diodes model by the extension term marked in the

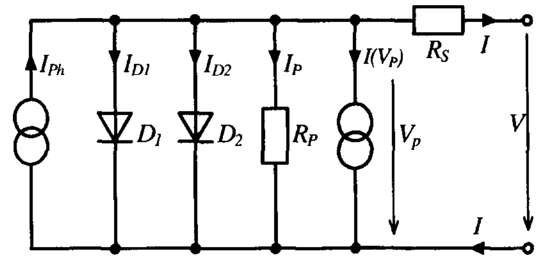

Fig. 1. Equivalent circuit of the solar cell, $I(V_P)$ generates the avalanche breakdown at high negative voltages.

equation above. This extension term can generate cell currents above the photocurrent. Such a current appears during the avalanche breakdown at high negative voltages (Miller, 1957; Bishop, 1988).

The photocurrent, the band gap and the diode saturation currents are temperature dependent. These parameters have to be changed if the temperature varies. The photocurrent is also proportional to the irradiance.

The electrical behavior of the solar cell is described over the whole voltage range. This is shown in Fig. 2 for a polycrystalline solar cell.

3. SIMULATION OF THE SOLAR CELL

In order to model the solar cell curve, the current I, for a given voltage V, must be computed individually for each value. Because the equation of the solar cell curve is not given in explicit form, numerical methods are normally used to determine the characteristic curve.

An equation for the solar cell $f(V, I) = 0$ is given in eqn (1). For a given voltage V the current I is determined by the root of eqn (1), where I is expected to be the single root. In order to determine the single root, it is suggested to use Newton–Raphson's method, described e.g. by Mathews (1987), as it offers considerable advantages over other methods. The main ideas of this algorithm will be described shortly. Starting with the initial value I_0, the following iteration is executed:

$$I_{i+1} = I_i - \frac{f(V, I_i)}{\dfrac{\partial f(V, I_i)}{\partial I}} \tag{2}$$

The iteration stops if a suitable condition is met. In the case above the absolute difference of two succeeding values of the iteration is used: $|I_{i+1} - I_i| < \epsilon$. The derivative of the solar cell equation can be given as shown below:

$$\begin{aligned} \frac{\partial f(V, I)}{\partial I} = &- \frac{I_{S1} R_S}{m_1 V_T} \exp\left(\frac{V + IR_S}{m_1 V_T}\right) - \frac{I_{S2} R_S}{m_2 V_T} \\ &\times \exp\left(\frac{V + IR_S}{m_2 V_T}\right) - \frac{R_S}{R_P} - 1 \\ &- aR_S\left(1 - \frac{n(V + IR_S)}{V + IR_S - V_{Br}}\right) \\ &\times \left(1 - \frac{V + IR_S}{V_{Br}}\right)^{-n} \end{aligned} \tag{3}$$

The Newton–Raphson algorithm can easily be implemented in a computer program. The

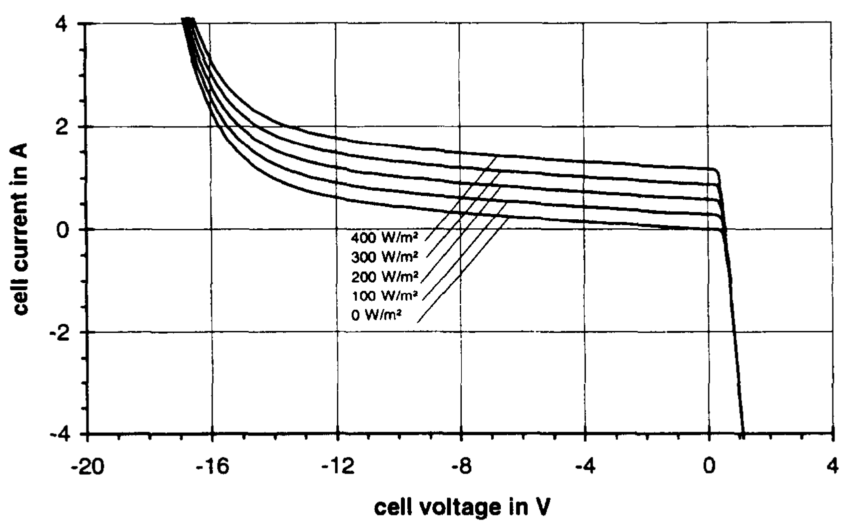

Fig. 2. Typical characteristic curves of a 10 × 10 cm polycrystalline solar cell at different irradiances (T = 300 K). The parameters are given in Fig. 3.

ton–Raphson algorithm has the advantage of a very quick, quadratic convergence for initial values near the root, so that a good solution can be calculated within a few iteration steps. In the proximity of the diode breakdowns difficulties occur. In this region the Newton–Raphson algorithm converges very slowly and can even diverge for badly chosen starting points.

To speed up the convergence, in this case, the bisection method can be used to determine an initial value for the Newton–Raphson method. Then, a more accurate solution can quickly be calculated by the Newton–Raphson method. The bisection method converges only linearly, but it cannot fail if the root is in the chosen interval. The interval is bisected and the part of the interval that does not contain the root is eliminated until the desired accuracy is reached.

Figure 3 shows a typical current–voltage characteristic of an unilluminated 10×10 cm polycrystalline solar cell over a wide range. The algorithms proposed above coincide with the measured points, proving to be an excellent method to describe the solar cell.

4. SOLAR GENERATOR MODEL

In the previous section it was shown how to calculate the characteristics of a solar cell. Now, this model can be used for various interconnections between solar cells, diodes, cables, and other components of solar generators.

In this section a method is described for the calculation of large networks. In addition, the characteristic curve of each component will be determined for each point of the generator curve. This is done to determine the power losses of a partly or fully shaded solar cell.

Kirchhoff's laws are applied to provide an equation system relating all currents and voltages in the network. A continuously varying system of nodes and meshes is difficult to describe for a computer. This is why a general model for an element interconnection is described as shown in Fig. 4.

The elements can be placed vertical ($A_{i,j}$) or horizontal ($B_{i,j}$) on a regular grid. Altogether there are z elements.

The following components can be used as elements:

- solar cell (two diodes equivalent circuit including negative diode breakdown description term);
- diode;
- resistance;
- ideal conductor (in this case $R_{\text{cond}} = 10^{-20}\ \Omega$);
- insulation resistance (in this case $R_{\text{insul}} = 10^{20}\ \Omega$)

etc.

It is also possible to use a whole assembly instead of a single component, for example a string of multiple solar cells. In this case the current–voltage curve and the derivative of the assembly must be known.

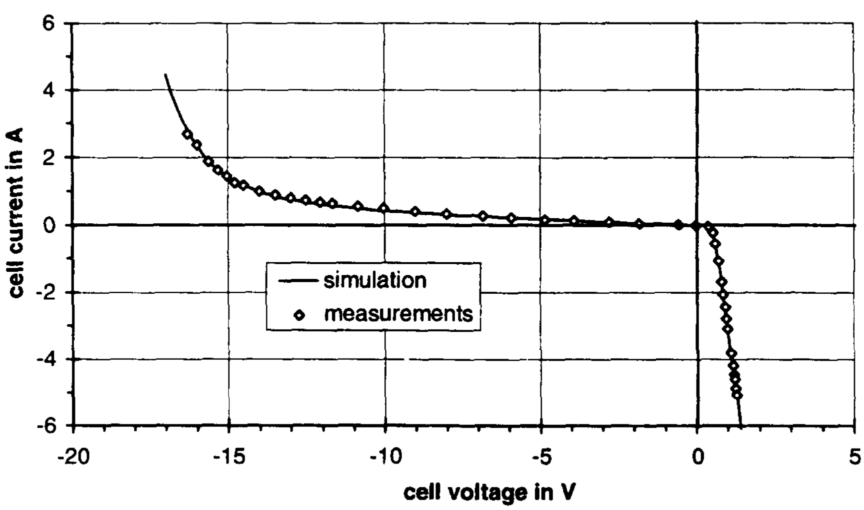

Fig. 3. Comparison between measurements and simulation of the characteristic curve of an unilluminated 10×10 cm polycrystalline solar cell (manufacturer ASE, Germany) with a high series resistance R_S due to line resistance. The following parameter set was used for the simulation: ($T = 300$ K; $I_{S1} = 3 \times 10^{-10}$ A; $m_1 = 1$; $I_{S2} = 6 \times 10^{-6}$ A; $m_2 = 2$; $R_S = 0,13\ \Omega$; $R_P = 30\ \Omega$; $V_{Br} = -18$ V; $a = 2,3 \times 10^{-3}\ \Omega^{-1}$; $n = 1,9$).

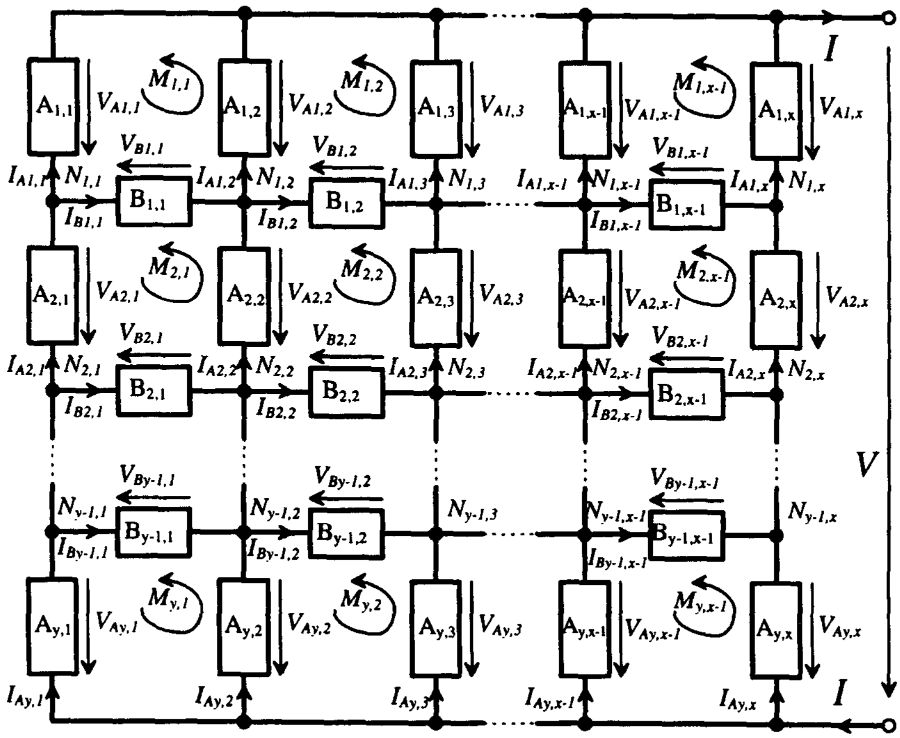

Fig. 4. General model for a connection of various elements in a photovoltaic assembly. (*A*: vertical elements, *B*: horizontal elements, *M*: meshes, *N*: nodes).

Each element is described by the mathematical relationship between current and voltage. These equations can be given in the following form:

$$f(V_{Ai,j}, I_{Ai,j}) = 0 \quad \text{and} \quad f(V_{Bi,j}, I_{Bi,j}) = 0$$

In this case the current for a given voltage has to be determined by a numerical method. For many elements (e.g. resistance) there is an explicit equation for the current:

$$I_{Ai,j} = g(V_{Ai,j}) \quad \text{and} \quad I_{Bi,j} = g(V_{Bi,j})$$

5. SIMULATION OF THE GENERATOR

The total voltage V is to be given for the determination of all characteristic curves. The relating total current I, all sub-voltages and sub-currents, can be calculated for this total voltage. This means the total voltage V can be interpreted as a known quantity and is kept constant for all calculations. For each sub-voltage the relating sub-current can be determined by the relations indicated above, so that the calculation of the sub-voltages is sufficient. Now, there are $z + 1$ unknowns. These are z sub-voltages of each element plus the total current I.

The vector $\mathbf{u}$ is the vector of the unknown sub-voltages and the unknown total current:

$$\mathbf{u}^{\mathrm{T}} = (V_{A1,1}, \ldots, V_{Ay,x}, V_{B1,1}, \ldots, V_{By-1,x-1}, I)$$

The total voltage is given, for example, by the following equation:

$$r_1(\mathbf{u}) = \sum_{i=1}^{y} V_{Ai,1} - V = 0 \qquad (4)$$

In the circuit there are altogether m meshes $M_{i,j}$, according to Kirchhoff's second law. The sum of the voltages in each mesh equals zero:

$$r_{2\ldots m+1}(\mathbf{u}) = V_{Ai,j} - V_{Bi,j} - V_{Ai,j+1} + V_{Bi-1,j} = 0 \qquad (5)$$

for $i = 1 \ldots y$; $j = 1 \ldots x - 1$ with $V_{Bi,j} = 0$ if $i = 0$ or $i = y$. For the total current I results the equation:

$$r_{m+2}(\mathbf{u}) = \sum_{j=1}^{x} I_{A1,j} - I = 0 \qquad (6)$$

Altogether there are n nodes $N_{i,j}$ in the circuit. According to Kirchhoff's first law, the sum of the currents equals zero.

$$r_{m+3\ldots m+n+2}(\mathbf{u}) = I_{Ai,j} = I_{Bi,j} - I_{Ai+1,j} - I_{Bi,j-1} = 0 \qquad (7)$$

for $i = 1 \ldots y-1$; $j = 1 \ldots x$ with $I_{Bi,j} = 0$ if $j = 0$ or $j = x$.

For the $z+1$ unknowns, represented by the vector **u**, $z+1$ independent equations $r_1(\mathbf{u}) \ldots r_{m+n+2}(\mathbf{u})$ are given. These equations form the non-linear equation system $\mathbf{r}(\mathbf{u})$.

$$\mathbf{r}(\mathbf{u}) = \begin{bmatrix} r_1(\mathbf{u}) \\ r_2(\mathbf{u}) \\ \vdots \\ r_{m+1}(\mathbf{u}) \\ r_{m+2}(\mathbf{u}) \\ r_{m+3}(\mathbf{u}) \\ \vdots \\ r_{m+n+2}(\mathbf{u}) \end{bmatrix} = \begin{bmatrix} \sum_{i=1}^{y} V_{Ai,1} - V \\ V_{A1,1} - V_{B1,1} - V_{A1,2} \\ \vdots \\ V_{Ay,x-1} - V_{Ay,x} + V_{By-1,x-1} \\ \sum_{j=1}^{x} I_{A1,j} - I \\ I_{A1,1} + I_{B1,1} - I_{A2,1} \\ \vdots \\ I_{Ay-1,x} - I_{Ay,x} - I_{By-1,x-1} \end{bmatrix} \qquad (8)$$

When using the solution vector **u** for a given total voltage V, all results of the equations of this equation system should be zero ($r_1(\mathbf{u}) = r_2(\mathbf{u}) = \ldots r_{m+n+2}(\mathbf{u}) = 0$). The root of the equation system, represented by the vector **u**, which satisfies the equation $\mathbf{r}(\mathbf{u}) = \mathbf{0}$, is to be found.

This equation system shall also be solved by applying numerical methods. The Newton–Raphson iteration requirement of a single equation with one unknown can be widened on the equation system. This results in:

$$\mathbf{u}_{i+1} = \mathbf{u}_i - (\mathbf{J}(\mathbf{u}_i))^{-1}\mathbf{r}(\mathbf{u}_i) \qquad (9)$$

Beginning with the starting vector $\mathbf{u}_0$ this iteration should be performed until the stopping condition $\|\mathbf{u}_{i+1} - \mathbf{u}_i\| < \epsilon$ is satisfied, ϵ having previously been determined. The vector $\mathbf{u}_{i+1}$, which satisfies the stopping condition also is the solution vector and includes the searched sub-voltages and the total current I.

The matrix $\mathbf{J}(\mathbf{u}_i)$ is called Jacobian matrix. The inverse of the Jacobian matrix $(\mathbf{J}(\mathbf{u}_i))^{-1}$ has to be determined for each iteration. The matrix is defined as shown below:

$$\mathbf{J}(\mathbf{u}_i) = \begin{bmatrix} \frac{\partial r_1(\mathbf{u}_i)}{\partial u_1} & \cdots & \frac{\partial r_1(\mathbf{u}_i)}{\partial u_{z+1}} \\ \vdots & \ddots & \vdots \\ \frac{\partial r_{z+1}(\mathbf{u}_i)}{\partial u_1} & \cdots & \frac{\partial r_{z+1}(\mathbf{u}_i)}{\partial u_{z+1}} \end{bmatrix} = \begin{bmatrix} \frac{\partial r_1(\mathbf{u}_i)}{\partial V_{A1,1}} & \cdots & \frac{\partial r_1(\mathbf{u}_i)}{\partial I} \\ \vdots & \ddots & \vdots \\ \frac{\partial r_{z+1}(\mathbf{u}_i)}{\partial V_{A1,1}} & \cdots & \frac{\partial r_{z+1}(\mathbf{u}_i)}{\partial I} \end{bmatrix} \qquad (10)$$

The partial derivatives of the mesh equations always equal ± 1 or 0. The derivatives of the node equations are more difficult to determine, especially if the current–voltage equations are not given in an explicit form. The derivatives, which are needed for the Jacobian matrix, can be calculated using the following expression:

$$\frac{\mathrm{d}I(U)}{\mathrm{d}U} = -\frac{\dfrac{\partial f(U,I)}{\partial U}}{\dfrac{\partial f(U,I)}{\partial I}} \qquad (11)$$

The Newton–Raphson method for equation systems shows similar features to those of the Newton–Raphson method for single equations. It can as well diverge at bad conditioned starting vectors and may obtain meaningless values. To avoid divergence problems the Newton–Raphson algorithm can be weakened by the following equation which was formulated by Press *et al.* (1992). This iteration, however, converges more slowly than the original Newton algorithm:

$$\mathbf{u}_{i+1} = \mathbf{u}_i - \lambda(\mathbf{J}(\mathbf{u}_i))^{-1}\mathbf{r}(\mathbf{u}_i) \quad 0 < \lambda \leq 1 \qquad (12)$$

The total characteristic curve can be determined by giving the total voltage V and calculating the total current I case by case using the iteration given above.

If sufficient values are calculated by the variation of the voltage V, the total curve can be described. The voltage range each element runs through is also obtained.

The described method allows one to determine all sub-voltages and the total voltage V for a given total current I as well. For this purpose, the current I in the vector **u** must be replaced by the total voltage V. In this case several partial derivatives in the Jacobian matrix are changed.

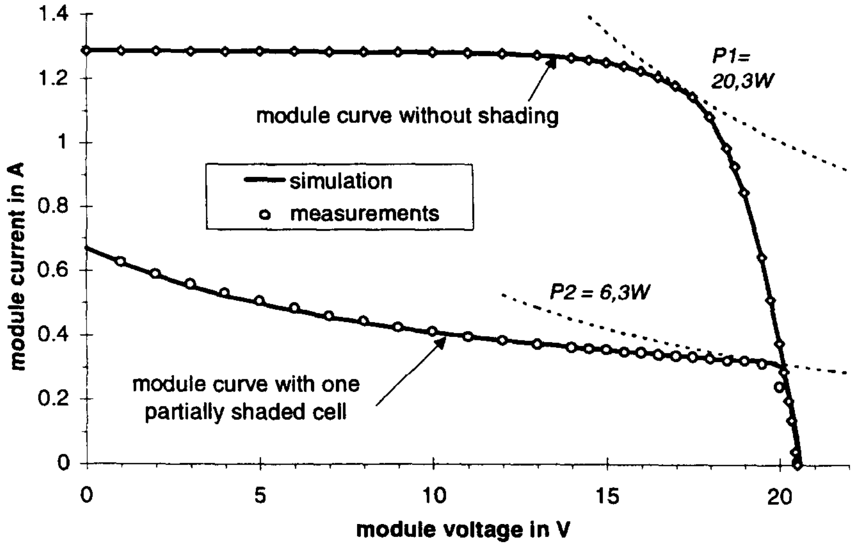

Fig. 5. Measurements and simulations for a solar module SM50 with 36 monocrystalline silicon solar cells with no bypass diodes. At the second curve 75% of one solar cell was shaded. The measurements were done under real sky conditions ($E = 407$ W/m^2, $T = 298$ K). The following parameter set was used for the simulation: ($I_{Ph} = 1,27$ A; $I_{S1} = 2,4 \times 10^{-10}$ A; $m_1 = 1$; $I_{S2} = 3,6 \times 10^{-6}$ A; $m_2 = 2$; $R_S = 14$ mΩ; $R_P = 225\ \Omega$; $V_{Br} = -41,5$ V; $a = 0,22 \times 10^{-3}\ \Omega^{-1}$; $n = 3$).

6. MODEL EVALUATION

Figure 5 shows a typical current–voltage characteristic of a photovoltaic module with 36 monocrystalline silicon solar cells without any bypass diodes at two different illumination situations. One curve presents the current–voltage characteristic of a uniform illuminated solar module under real sky conditions. The other curve shows the current–voltage characteristic of the same module at the same irradiance and temperature, but 75% of one solar cell of the module are shaded. The simulated curve of the photovoltaic module coincides just as well as the simulated curve of the single solar cell in Section 3 with the measured points. Therefore, the described method for the photovoltaic generator is perfectly suited to obtain simulations for the current–voltage characteristics.

The influence of module shading on the module performance can also be seen in Fig. 5. The performance loss is 70% although only 2% of the module area is shaded. Part of the performance difference has to be dissipated by the shaded cell. To avoid cell damaging the module manufacturers integrate bypass diodes over cell strings of 16 up to 24 cells. Figure 6 shows that the module performance loss can only be reduced insignificantly by bypass diodes over large cell strings. In the case of the 75% shaded cell the performance loss decreases from 70 to 55% by the use of bypass diodes over 18 cells. Only separate bypass diode over every cell can minimize the performance losses. Therefore, Green *et al.* (1981, 1984) and Shepard and Sugimura (1984) proposed to integrate bypass diodes into solar cells. Figure 7 shows a simulation of the same module used in Fig. 6 with bypass diodes over different numbers of solar cells. Again 75% of one solar cell are shaded. The performance losses can be reduced to 5% if a bypass diode is used over every cell.

7. CONCLUSIONS

A model for the description of the total characteristic curve for a solar cell, based on the two diodes model and the model of Bishop (1988) is described. Numerical methods are necessary to determine the current–voltage curve. Some well-known numerical algorithms and their implementation are described. Furthermore, a general model for the determination of a solar generator curve as well as all sub-voltages and sub-currents of the solar generator are given. The suitable algorithms for the solution of the equation system are introduced for this model.

By analysing the sub-curves, statements regarding possible power losses at mismatched or shaded solar cells can be made. This is necessary to minimize the power losses resulting from shading, and to avoid the damaging of

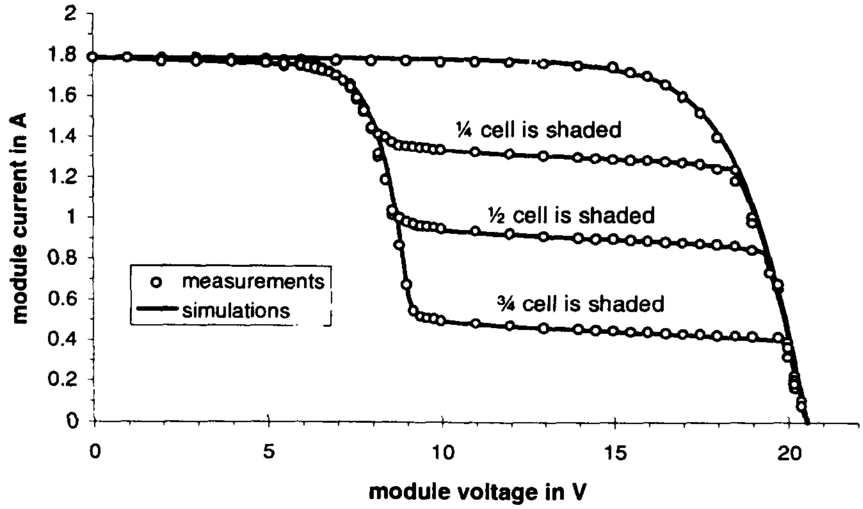

Fig. 6. Measurements and simulations for a solar module SM50 with 36 monocrystalline silicon solar cells with two bypass diodes. One cell was shaded differently. The measurements were done under real sky conditions ($E = 574$ W/m^2, $T = 300$ K). The following parameter set was used for the simulation: (I_{Ph} = 1, 79 A; $I_{S1} = 3, 3 \times 10^{-10}$ A; $m_1 = 1$; $I_{S2} = 7, 8 \times 10^{-6}$ A; $m_2 = 2$; $R_S = 14$ mΩ; $R_P = 150\ \Omega$; $V_{Br} = -30$ V; $a = 8 \times 10^{-4}\ \Omega^{-1}$; $n = 1, 9$).

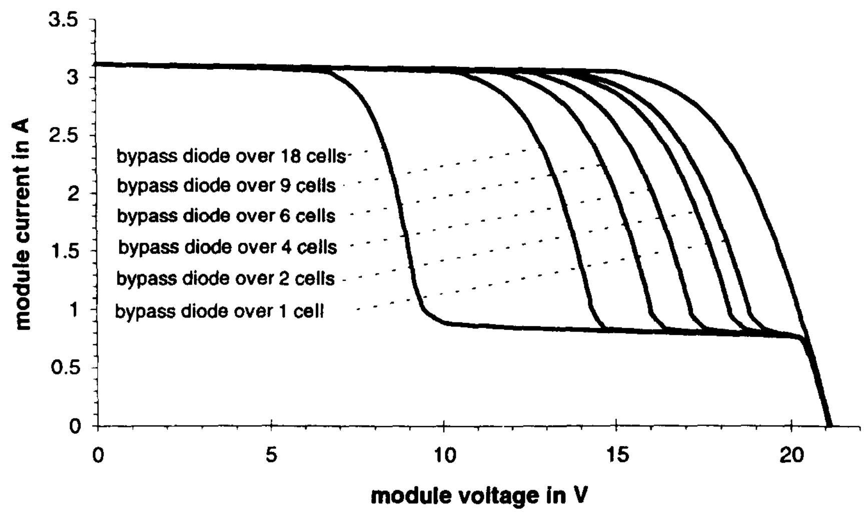

Fig. 7. Simulations for the same module as used in Fig. 6. The bypass diodes were connected over different cell string sizes. 75% of one cell was shaded. As parameters $E = 1000$ W/m^2, $T = 300$ K, $I_{Ph} = 3, 11$ A were used. The other parameters were the same as used for Fig. 6.

solar cells by hot spots during high power losses. The performance losses can drastically be reduced by using a bypass diode over every cell. This should be an important aspect to pick up the shading problem again and to think about new shadow-tolerant modules for terrestrial applications.

NOMENCLATURE

ϵ exactness for stopping iteration
λ factor in the modified Newton iteration
a correction factor ($a < 1\ \Omega^{-1}$)
$A_{i,j}$ vertical element (i, j running position index)
$B_{i,j}$ horizontal element (i, j running position index)
f function
i index
I current of the solar cell or the solar generator
$I_{Ai,j}$ current at element $A_{i,j}$
$I_{Bi,j}$ current at element $B_{i,j}$
I_{Ph} photocurrent
I_{S1} saturation current of the first diode
I_{S2} saturation current of the second diode
$I(V_p)$ current generated for the diode breakdown at high negative voltages
j index
$\mathbf{J(u)}$ Jacobian matrix
m number of meshes; $m = y(x-1)$
m_1 ideality factor of the first diode
m_2 ideality factor of the second diode
$M_{i,j}$ Kirchhoff mesh (i, j running position index)

n avalanche breakdown exponent ($n = 1 \ldots 10$)
n number of nodes; $n = x(y-1)$
$N_{i,j}$ Kirchhoff node (i, j running position index)
$\mathbf{r}(\mathbf{u})$ system of nonlinear equations
$r_i(\mathbf{u})$ partial function of $\mathbf{r}(\mathbf{u})$
R_P parallel or shunt resistance
R_S series resistance
T temperature
$\mathbf{u}$ vector of unknowns
U_0 starting vector for the iteration
u_i element of the vector $\mathbf{u}$
V voltage of the solar cell or the solar generator
$V_{Ai,j}$ voltage at element $A_{i,j}$
$V_{Bi,j}$ voltage at element $B_{i,j}$
V_{Br} breakdown voltage ($V_{Br} \approx -15\text{ V} \ldots -40\text{ V}$)
V_P voltage over the parallel resistance R_P
V_T temperature voltage
x number of horizontal elements of a row
y number of vertical elements of a column
z number of all elements (vertical and horizontal); $z = 2xy - x - y + 1 = m + n + 1$

BIBLIOGRAPHY

Abete, A., Barbisio, E., Cane, F. and Demartini, P. (1990) Analysis of photovoltaic modules with protection diodes in presence of mismatching. *21st IEEE PV Specialists Conf.*, pp. 1005–1010, Kissimimee, U.S.A.

Engeln-Müllges, G. (1990) Formelsammlung zur Numerischen Mathematik mit C-Programmen. BI-Wissenschaftsverlag, Mannheim.

Quaschning, V. and Hanitsch, R. (1995) Shade calculations in photovoltaic systems. *ISES Solar World Congress*, Harare, Zimbabwe.

Quaschning, V. and Hanitsch, R. (1995) Quick determination of irradiance reduction caused by shading at PV-locations. *13th European Photovoltaic Solar Energy Conf.*, Nice France.

Rauschenbach, H. S. (1971) Electrical output of shadowed solar arrays. *IEEE Trans. on Electron Devices*, **18**, 483-490.

Stoer, J. (1993) *Numerische Mathematik 1*. Springer, Berlin.

Suryanto Hasyim, E., Wenham, S. R. and Green, M. A. (1986) Shadow tolerance of modules incorporating integral bypass diode solar cells. *Solar Cells* **19**, 109–122.

Swaleh, M. S. and Green, M. A. (1982) Effect of shunt resistance and bypass diodes on the shadow tolerance of solar cell modules. *Solar Cells* **5**, 183-198.

Wagdy, R. A. (1989) Partial shadowing protection without diodes. *Solar Cells* **26**, 227–239.

REFERENCES

Bishop, J. W. (1988) Computer simulation of the effects of electrical mismatches in photovoltaic cell interconnection circuits. *Solar Cells* **25**, 73–89.

Green, M. A., Gauja, F. and Yachamanankul, W. W. (1981) Silicon solar cells with integrated bypass diodes. *Solar Cells* **3**, 233–244.

Green, M. A., Hasyim, H. S., Wenham, S. R. and Willison, M. R. (1984) Silicon solar cells with integrated bypass diodes. *17th IEEE Photovoltaic Specialists Conf.*, pp. 513–517, Kissimimee, U.S.A.

Mathews, J. H. (1987) *Numerical Methods for Computer Science, Engineering and Mathematics*. Prentice Hall, NJ.

Miller, S. L. (1957) Ionization rates for holes and electrons in silicon. *Phys. Rev.* **105(4)**, 1246–1249.

Overstraeten, R. J. and Mertens, R. P. (1986) *Physics, Technology and Use of Photovoltaics*. Adam Hilger, Bristol.

Press, W. H., Teukolsky, S. A., Vetterling, W. T. and Flannery, B. P. (1992) *Numerical Recipes in C*. Cambridge Univ. Press.

Rauschenbach, H. S. (1980) *Solar Cell Array Design Handbook*. Van Nostrand Reinhold, New York.

Shepard, N. F. and Sugimura, R. S. (1984) The integration of bypass diodes with terrestrial photovoltaic modules and arrays. *17th IEEE Photovoltaic Specialists Conf.*, pp. 676–681, Kissimimee, U.S.A.